LA-UR-82-1774

CONF-811117--7

Los Alamos National Laboratory is operated by the University of California for the United States Department of Energy under contract W-7405-ENG-36

LA-UR--82-1774

DE82 019578

TITLE: MULTIPLE-SHOT ULTRAVIOLET LASER DAMAGE RESISTANCE OF NONQUARTERWAVE REFLECTOR DESIGNS FOR 248 NM

AUTHOR(S): Brian E. Newnam
Stephen R. Foltyn
L. John Jolin

SUBMITTED TO: Proceedings of 1981 Boulder Damage Symposium

MASTER

DISTRIBUTION OF THIS DOCUMENT IS UNLIMITED

DISCLAIMER

Los Alamos

Los Alamos National Laboratory
Los Alamos, New Mexico 87545

FORM NO 836 R4
ST NO 2629 5/81

Multiple-Shot Ultraviolet Laser Damage Resistance of Nonquarterwave Reflector Designs for 248 nm

Brian E. Newnam, Stephen R. Foltyn, and L. John Jolin

University of California, Los Alamos National Laboratory, Los Alamos, NM 87545

and

C. K. Carniglia

Optical Coating Laboratory, Inc., Santa Rosa, CA 95402

The damage resistance of multilayer dielectric reflectors designed for 248 nm has been substantially increased by use of nonquarterwave (QW) thicknesses for the top few layers. These designs minimize the peak standing-wave electric field in the high-index layers, which have proven to be weaker than the low-index components.

Previous damage tests of infrared- and visible-wavelength reflectors based on these designs have produced variable results. However, at the ultraviolet wavelength of 248 nm, 99% reflectors of Sc_2O_3, MgF_2, and SiO_2 strongly demonstrated the merit of non-QW designs. Four sets of reflectors of each of four designs (all QW thickness; one modified-pair substitution; two modified-pair substitution; one modified pair plus an extra half-wave layer of Sc_2O_3) were tested for damage resistance with a KrF laser operating at 35 pps with a pulsewidth of 8 ns and spot-size diameter of 0.6 mm. Each of 50 sites were irradiated for 1000 shots or until damage occurred.

On the average, the reflectors with one-modified-thickness pair had a 50% higher threshold (10 of 10 sites survived) than the all-quarterwave design. Addition of a second modified-layer pair resulted in no further increase in threshold but the saturation fluence (10 of 10 sites damage) was 110% higher. Reflectors with an additional half-wave of Sc_2O_3 had lower thresholds of the order of 10% as expected. The thresholds correlated best with peak-field models, whereas the best model correlating the saturation fluences involved the sum of the upper two scandia layer thicknesses.

Key words: Damage thresholds; electric-field suppression; multiple shots; nanosecond pulses; nonquarterwave designs; scandium oxide; standing-wave electric fields; thin films; ultraviolet reflectors.

1. Introduction

In recent years, the anticipated correlation of peak standing-wave (SW) electric field with laser damage of multilayer dielectric reflectors has been under repeated scrutiny [1-7]. Damage studies of various coating designs have been conducted at both Los Alamos and Livermore National Laboratories in cooperation with commerical vendors, primarily Optical Coating Laboratory, Inc. (OCLI). The results of these previous investigations have been variable. Possible reasons for these variations are discussed in Section 6.

Previous correlation of the damage threshold with SW-field patterns for the ultraviolet wavelength of 266 nm [8] provided the motivation for the present study at 248 nm. Here, we examined the use of special reflector designs in which the upper few layers had nonquarterwave (QW) thicknesses. While maintaining high reflectance, this non-QW design modification minimizes the peak SW field in the top high-index layers, which have proven to be weaker than the low-index layer materials. Figure 1 allows a comparison of the field patterns for the standard all-QW reflector and for an optimized suppressed-field design. The latter is obtained in two steps. First, a low-index layer is added to the standard QW stack, but its optimum thickness is such that the electric field at its outer surface exactly equals that at the second H-L interface. Then sufficient thickness of the high-index film is added to obtain a null field at its outer surface, thereby maximizing the reflectance. Additional pairs of layers can be added according to the same principles.

Success of the non-QW design in realizing higher damage thresholds requires that the ratio of the thresholds for the high- and low-index films be substantially greater than unity. Especially for ultraviolet laser wavelengths, suppression of the peak electric field in the high-index layers is expected to be advantageous for at least three reasons. (1) the density of absorbing film defects increases with decreasing wavelength [9], (2) homogeneous absorption increases rapidly near the uv band edge, and (3) multiphoton absorption becomes a probably contributing damage mechanism.

2. Test Specimens

2.1 Reflector Design

Four different 22-layer reflector designs were coated using three materials: scandium oxide (Sc_2O_3), magnesium fluoride (MgF_2), and silicon dioxide (SiO_2). To preclude stress-induced crazing, the initial layers were composed of five pairs of Sc_2O_3/SiO_2 over which six pairs of Sc_2O_3/MgF_2 and half-wave (HW) thick MgF_2 overcoat were deposited. The four different designs shown in table 1 differed only in the thicknesses of the outer pairs of layers. Design A was the standard all-QW stack. The layer thicknesses of Designs B and D were chosen to minimize the peak SW field in the scandia layers as specified by Gill et al. [4]:

$$\text{Low-index layers:} \quad \sin \theta_{2i-1} = [iN^2-(i-1)]^{-1/2}, \; \theta_{2i-1} > \pi/2 \tag{1}$$

$$\text{High-index layers:} \quad \tan \theta_{2i} = N[i(N^2-1)]^{-1/2}, \; \theta_{2i} < \pi/2 \tag{2}$$

where $\theta < i \leq m$ (m being the number of pairs of non-QW layers), $N = n_H/n_L$, and $\theta_i = 2\pi n_i d_i/\lambda$. The subscripts, L and H, refer to the low- and high-index layers and d is the film thickness. Similar expressions have also been derived by Apfel [10]. Design C was the same as B except the top scandia layer was an additional HW thicker. This design was included not to increase damage resistance but to provide insight into the damage mechanism.

2.2 Reflector Fabrication

Four sets of the above designs were deposited in two essentially identical coating runs, using four suprasil-2 substrates and four BK-7 glass substrates per run. The suprasil substrates (50.8 mm diam) had surface roughness of ~10 Å rms, and the BK-7 substrates (50.8 and 38.1 mm diam) had a low-scatter bowlfeed polish for which 3 - 5 Å rms roughness is typical. The coatings were deposited at a substrate temperature of 150° C for both runs. Flip masking was used so that all of the scandia/silica layers and all QW scandia/MgF_2 layers were common to all parts. Additionally, the 377-L, 149-H layers were common to spindles B, C, and D, and the HW MgF_2 overcoat was common to all parts.

2.3 Spectral Performance

As can be seen in table 2 and figure 2, the spectral performance of the actual reflectors was very close to the theoretical design values. At 248 nm the reflectance generally exceeded 99%. The parts of Design C were about 0.5% lower as expected due to the added absorption in the thick scandia layer. The extinction coefficient k of the Sc_2O_3 was measured to be 0.002 ± 0.005. The k values of MgF_2 and SiO_2 did not exceed zero within this precision.

2.4 Electric-field Distributions

The internal SW electric-field distributions for each reflector design are shown in figure 3. The fields were computed numerically with the assumption of no absorption and are normalized to the incident field E_0. The thicknesses, peak fields, and linear absorption in the upper layers are listed in table 3. The first two quantities can be computed from analytical expressions derived previously [4, 10]. The linear absorption was obtained by integration over each layer of thickness t by

$$A = (4\pi nk/\lambda) \int_0^t |E(z)/E_0|^2 dz \tag{3}$$

Table 1 248-nm Reflector Designs

A. Quarterwave stack

$SUB/(HL')^5 \; (HL)^5H \; LL$

248 248 248

B. 1 Pair Suppressed E-Field

$SUB/(HL')^5 \; (HL)^4H \; L \; H \; LL$

248 248 377 149 248

C. 1 Pair Suppressed E-Field with Scandia Half-Wave

$SUB/(HL')^5 \; (HL)^4H \; L \; H \; LL$

248 248 377 645 248

D. 2 Pairs Suppressed E-Field

$SUB/(HL')^5 \; (HL)^3H \; L \; H \; L \; H \; LL$

240 248 377 149 404 122 248

Table 2. Measured Performance of 248-nm Reflectors

	Spindle	R_{peak}	R_{248}	λ_o(nm)[a]	λ_{peak}(nm)
A.	Theoretical[b]	0.993	0.993	248	244
	603-1727	0.996	0.992	244	251
	603-1728	0.990	0.989	242	249
B.	Theoretical[b]	0.994	0.994	250	247
	603-1727	0.993	0.989	245	251
	603-1728	0.991	0.991	243	248
C.	Theoretical[b]	0.988	0.988	249	248
	603-1727	0.990	0.982	248	251
	603-1728	0.988	0.988	246	248
D.	Theoretical[b]	0.993	0.993	252	250
	603-1727	0.991	0.990	247	251
	603-1728	0.990	0.990	246	248

[a]The wave number average of the 80% points.

[b]Based on the nondispersive refractive indices of the materials as follows:

		n	k
H:	Sc_2O_3	2.05	0.002
L:	MgF_2	1.40	0.0
L':	SiO_2	1.50	0.0

3. Laser Damage Test Conditions

The experimental arrangement and test procedures have been described previously [11, 12] and in the companion paper in this proceedings by Foltyn et al. [13]. The laser test parameters are given in table 4. In addition to the tests at 35 pps, one of the four sets of reflectors was also tested at 2 pps.

4. Experimental Results

4.1 Irradiation at 35 pps

The results for one of the four sets of reflectors are plotted in figure 4. A least-squares-linear fit to the data is generally quite good and differs only slightly from a logarithmic curve fit which is motivated by a spot-size-dependent damage model [13]. The starred data points on the abscissa indicate the fluence levels for which a slow, 26-mm scan of the laser beam (at 35 pps) produced no additional damage. The damage threshold is defined as the maximum laser fluence at which 0 of 10 test sites damaged. Extrapolation of the linear curve to the 10 of 10 sites damage level determines the "saturation fluence." This latter quantity is the minimum fluence necessary to produce damage of every test site and as discussed earlier [13], is thought to be dependent on the laser spot size. For the data exhibited in figure 4, it is obvious that both the one- and two-pair non-QW designs yielded significantly higher damage thresholds and saturation fluences. On the other hand, the reflector with an additional HW thickness of scandia had nearly the same threshold as the all-QW reflector, and its saturation fluence was only slightly greater than its threshold. Table 5 lists the thresholds for all four sets of reflectors. Not surprisingly, the results for the corresponding reflectors of the different sets reveal only slight differences in magnitudes. In every case but one, the thresholds of the two optimized designs surpassed those of the all-QW reflectors.

The influence of substrate material and/or surface polish was very slight. The mean values for the thresholds and saturation fluences for reflectors on suprasil 2 were about 10% greater than the mean values for reflectors on BK-7 glass. Neither did the results for the two coating runs differ much. Run 1727 yielded reflectors about 10% more damage resistant than Run 1728. While these small differences are considered real, their magnitudes are practically negligible.

Table 3. Design and Theoretical Performances of 248-nm Reflectors[a]

Design	A QW Stack	B One Pair Suppressed E-field	C One Pair Suppressed E-field +λ/2 H	D Two Pair Suppressed E-field
Overcoat (MgF_2)				
Thickness[b]	2.0	2.0	2.0	2.0
Peak Field[c]	2.03	2.03	2.03	2.03
Layer 21 (Sc_2O_3)				
Thickness[b]	1.0	0.60	2.60	0.49
Peak Field[c]	0.95	0.62	0.95	0.46
Absorption	0.0030	0.0009	0.0068	0.0005
Layer 20 (MgF_2)				
Thickness[b]	1.0	1.52	1.52	1.63
Peak Field[c]	0.95	1.33	1.33	1.51
Layer 19 (Sc_2O_3)				
Thickness[b]	1.0	1.0	1.0	0.60
Peak Field[c]	0.44	0.62	0.62	0.46
Absorption	0.0014	0.0019	0.0019	0.0006
Layer 18 (MgF_2)				
Thickness[b]	1.0	1.0	1.0	1.52
Peak Field[c]	0.44	0.62	0.62	0.98
Layer 17 (Sc_2O_3)				
Thickness[b]	1.0	1.0	1.0	1.0
Peak Field[c]	0.21	0.29	0.29	0.46
Absorption	0.0006	0.0009	0.0009	0.0014
Total Absorbance	0.0056	0.0045	0.0105	0.0039
Reflectance	0.9935	0.9941	0.9882	0.9940

[a]Based on the refractive indices given in table 2.

[b]Thicknesses are given in terms of quarterwaves at 248-nm.

[c]Peak field is the time average square of the electric field relative to the incident field.

Table 4. Laser Test Parameters

Wavelength	248 nm
Pulsewidth	8 ns (FWHM)
Spot-size Diameter	0.6 mm, Mean
Repetition Rate	35 pps, (and 2 pps)
Sites Irradiated	10 at each of 5 fluence levels
Shots Per Site	1000

Table 5. Experimental Damage Thresholds (J/cm^2)

Coating Run	Substrate	Coating Design			
		All QW	One Pair Non-QW	Two Pair Non-QW	One Pair Non-QW +HW Sc_2O_3
603-1727	Suprasil 2	3.0,[a] (4.9)[b]	4.4, (6.7)	4.4, (11.5)	2.5, (3.1)
603-1727	BK-7	3.0, (5.6)	5.6, (6.8)	4.7, (10.3)	2.5, (2.9)
603-1728	Suprasil 2	3.0, (5.1)	4.2, (7.2)	4.9, (9.6)	3.0, (3.4)
603-1728	BK-7	2.6, (3.8)	3.4, (6.6)	2.6, (10.0)	2.7, (3.1)

[a]Threshold of damage ≡ maximum fluence at which none of 10 sites irradiated damaged.

[b]Saturation fluence ≡ minimum fluence to damage all 10 of 10 sites irradiated.

As has been demonstrated repeatedly in the last decade of damage research, a result may not be reproducible when retested due to many factors in real materials. Thus, it is the average or trend revealed by repeated tests of a particular design concept or manufacturing procedure that is of most value. We have tried to address this issue in the present work by testing four sets of these reflectors fabricated in two coating runs. From table 4 we computed the average thresholds for each design and present these in table 6. To further clarify the results, we also present the same information in figure 5.

Clearly the optimized non-QW designs have superior thresholds (higher by 40 to 50%) and saturation fluences (40 to 100% higher). Not unexpectedly, the additional HW scandia thickness resulted in a slightly (significantly) decreased threshold (saturation fluence).

4.2. Irradiation at 2 pps

The test results for the set of reflectors tested at both 2 pps and 35 pps are plotted in figure 6. On the average, the thresholds and saturation fluences for these tests differed by 5% or less. Furthermore, the 2-pps tests allowed us to identify the shot number at which damage occurred. (This was difficult to accurately quantify at 35 pps.) We observed that either a test site damaged within 25 shots or it survived the standard 1000-shot test. Further, for nearly 75% of those sites exhibiting damage, failure occurred on the first shot. This aspect is adequately discussed in the preceding paper by Foltyn et al. [13].

5. Analysis

The experimental results positively reveal the merit of using the suppressed electric-field principle to increase the damage resistance of laser reflectors. It is still conceivable, however, that minimizing the peak field in the scandia layers is serendipitous. That is, there may be another condition that is simultaneously optimized that involves the primary damage mechanism. In this section, we compare our results with the theoretical predictions of various models for laser damage.

First, we can state that the low-index layers of MgF_2 are not the sites of initial breakdown. For each of the four reflector designs, the MgF_2 overcoat thickness was the same, and the peak and average fields were also the same (see table 3). Yet the damage thresholds varied considerably. We considered then, damage models involving initial failure in the scandia layers. (Only for the two-pair non-QW design was initial damage in the MgF_2 indicated, as discussed below.)

The obvious models for damage involve one or more of the following parameters: the peak SW electric field, the average field, absorption, or layer thickness. We have considered ten different possible models. Model 1 is that damage thresholds are inversely proportional to the peak SW electric field. This is consistent with damage via absorption, both linear and nonlinear, and electron avalanche. This dependence between energy linearly absorbed per unit volume and the field squared is given by

$$\epsilon_a(\mathrm{J/cm^3}) = n\alpha|E(z)/E_0^+|^2\epsilon_0 \qquad (4)$$

where $\alpha = 4\pi k/\lambda$ and ε_o is the laser fluence in J/cm². Model 2 predicts initial failure at film interfaces having the largest SW field. Possibly, defects could be trapped at these boundaries. Model 3 has damage dependent on the maximum average field in any one layer. This relates to the total absorption within a layer of thickness, t, by the expression

$$|E/E_o^+|^2_{av} = A/n\alpha t \quad . \qquad (5)$$

Model 4 involves the average field in the top scandia layer which could be most susceptible to atmospheric contamination.

Model 5 involves the maximum total linear absorption in any one layer, and Models 6 and 7 involve the total absorption in the top scandia layer and upper two scandia layers, respectively. Model 8 involves the sum of the linear absorptions within all the scandia layers.

Model 9 predicts that the threshold will increase with decreasing thickness of the top scandia layer. This is consistent with the number of absorbing defects the laser beam would encounter. Model 10 is the same, except it involves the sum of the thicknesses of the upper two scandia layers, which for the designs tested, were the only ones that were varied.

In figures 7-10 we present graphs of the mean thresholds versus the parameters unique to four of the models. The mean threshold is the average for the four reflectors of identical design and the vertical bars are the standard deviations from these mean values. A linear least-squares-fit is drawn through each plot and the coefficient of determination, r^2, was computed. A value of 1.000 for r^2 would be a perfect fit. Exponential, logarithmic and power curves did not fit the data as well as straight lines.

The four models selected for illustration here had values of r^2 coefficients very close to 1.00. The reader can verify this by examining table 7 where the statistical results for all the models are summarized. Since the mean threshold (no sites damage) for the two-pair non-QW design was slightly lower than for the optimized one-pair design (4.15 compared to 4.4 J/cm²) the linear fits for all ten models initially were poor with $r^2 < 0.90$. An obvious hypothesis is that threshold damage initiated in the MgF_2 overcoat for this design. This is reasonable since the field in the high-index layers can be suppressed to advantage only to the degree that the low-index films have higher damage resistance. With this hypothesis (II), the r^2 coefficients increased markedly for most of the lines drawn through the thresholds. In particular, Models 1 (peak field) and 6 (linear absorption in top scandia layer) provided excellent fits ($r^2 \sim 0.99$) as is apparent in figures 7 and 10.

The very poor correlation of Model 2 (maximum field at a film interface) deserves special mention since it has been previously considered as plausible [5]. Reflectors of Design C with peak field in the interior of the thick scandia layer had thresholds in direct opposition to this model. Apparently film interfaces are not significantly more damage prone than interior material.

For the saturation fluences, a different set of models was most consistent with the data. The best fit was provided by Models 10, 6, and 5 in descending order. Model 10 ($r^2 = 0.99$), predicting higher thresholds for designs with thinner layers, is consistent with failure by beam interaction with a particular class of coating defects. Presumably, the thicker the films, the greater the number of these defects that will be encountered. Walker et al. [9] also reported a similar increase in damage resistance of thinner single-layer films. However, their definition of damage threshold (midway between our threshold and saturation fluence definitions) was the traditional one

Table 6 Experimental Results

Four-Set Average of Four Designs of 248-nm Reflectors

Design	Threshold J/cm²	% Change	Saturation Fluence J/cm²	% Change
All QW	2.9 ± 0.2	--	4.85 ± 0.6	--
One-pair Non-QW	4.4 ± 0.9	+ 50%	6.8 ± 0.3	+ 40%
Two-pairs Non-QW	4.2 ± 1.1	+ 40%	10.4 ± 0.8	+ 110%
One-pair Non-QW + HW Sc_2O_3	2.7 ± 0.1	- 10%	3.1 ± 0.2	- 35%

Table 7. Statistical Analysis of Damage Models

Model/Hypothesis	Coefficient r^2 for Linear Fit		
	Thresholds		Saturation Fluences
	I	II	I
1. Peak field	0.71	0.99	0.95
2. Maximum field at interface	0.35	0.16	0.52
3. Maximum field average in any one layer	0.65	0.86	0.88
4. Average field in top Sc_2O_3 layer	0.69	0.93	0.91
5. Maximum linear absorption in any one layer	0.77	0.84	0.97
6. Total linear absorption in top Sc_2O_3 layer	0.72	0.99_6 [a]	0.98 [a]
7. Total linear absorption in top two Sc_2O_3 layers	0.47	0.87	0.95
8. Total absorption in stack	0.75	0.69	0.86
9. Thickness of top Sc_2O_3 layer	0.84	0.86	0.92
10. Thickness sum of top two Sc_2O_3 layers	0.64	0.71	0.99

[a] Linear fit predicts a threshold of more than 2.0 J/cm^2 at infinite absorption; see text.

Hypothesis I. Initial damage in Sc_2O_3 films.

Hypothesis II Same as I, except damage initiates in the HW MgF_2 overcoat only for the two-pair non-QW design.

Particular comment is necessary for Model 6 as illustrated in figure 9. Although the linear fits were exceptionally good ($r^2 = 0.99_6$ and 0.98), the projected thresholds for infinite absorption were greater than 2 J/cm^2. This appears to be a nonphysical result since the lines should pass close to the origin.

By use of the slope of the linear fit for the thresholds of figure 7, we computed the mean value of the peak-field threshold for Sc_2O_3 to be 0.36 MV/cm. For the two-pair modified design in which damage is assumed to initiate in the HW MgF_2 overcoat, a mean value of 0.63 MV/cm was computed. The ratio of these field thresholds is 1.76, which is sufficiently large to motivate the present suppressed-field reflector designs.

Summarizing this section, mean threshold data were most consistent with the peak-field Model 1, and the saturation fluence data were most consistent with the top two scandia layer thickness sum of Model 10. The thresholds for two-pair non-QW designs fell markedly below the linear curve fits suggesting initial failure of an MgF_2 layer (presumably the HW overcoat). Finally, the use of all of the models (except Model 2) evaluated here supported the observed trend of increasing thresholds and saturation fluences with decreasing peak and average fields, absorption, and layer thicknesses.

6 Discussion of Past Experience

As mentioned in the introductory section, previous use of the suppressed-field principle has not always correlated well with damage resistance.

The Los Alamos group, using 20- to 30-ps pulses at 1064 and 532 nm [1-4] and 20-ns pulses at 266 nm [8] often found a definite correlation. However, Livermore and CO/LI researchers using 150-ps and 1-ns pulses at 1064 nm found no firm evidence of the SW-field influence on damage threshold [5-7].

There are several possible explanations for the different observations. First, at the damage threshold fluence, the peak electric field for 20- to 30-ps pulses is much higher than for nanosecond pulses and so field-dependent mechanisms are emphasized. Secondly, whereas the internal SW-field pattern is essentially constant during the picosecond laser pulses, thermal diffusion of deposited energy away from SW peaks can decrease the temperature extremes arising from energy absorbed over nanosecond times. Thirdly, individual defects randomly distributed throughout the films are apparently the first sites to damage. These defects would tend to mask any SW-field threshold correlation. However, for picosecond pulses the density of damageable defects is apparently greatly increased as evidenced by an absence of any spot-size dependence of damage [2]. Thus, the films become essentially uniform in susceptibility to laser damage and the SW fields become manifest. Fourthly the positive correlation (even for nanosecond tests) with ultraviolet wavelengths is consistent with a uniform density of coating defects argument. The density of susceptible defects increases as the wavelength approaches the absorption edge as reported by Walker et al. [9].

The successful use of suppressed peak fields to increase the damage resistance of 248-nm reflectors is consistent with previous research. Even greater advantage is anticipated at shorter wavelengths.

7. Summary

Application of the principle of suppression of the peak electric field in the top high-index layers has resulted in substantially increased damage resistance for multilayer dielectric reflectors of $Sc_2O_3/MgF_2/SiO_2$ designed for 248 nm. On the average, the reflectors with one pair of optimized-thickness layers had 50% higher thresholds (survival of 10 of 10 sites) than the all-QW design. Addition of a second pair of optimized non-QW layers resulted in no further increase in threshold, but the saturation fluence (damage of 10 of 10 sites) was 110% higher. A model of damage resistance inversely proportional to the electric-field peak in the high-index (scandia) layers provided the best fit to the threshold data. Also this model was the only one (out of ten) to accurately predict the threshold for the special test reflector incorporating an extra HW thickness in the top scandia layer. The saturation fluences correlated best with the sum of the thicknesses of the upper two scandia layers which is consistent with damage of a special class of film defects.

8. References

[1] Newnam, B. E.; Gill, D. H. Laser damage resistance and standing-wave fields in dielectric coatings. J. Opt. Soc. Am. 66:166, 1976.

[2] Newnam, B. E.; Gill, D. H.; Faulkner, G. Influence of standing-wave fields on the laser damage resistance of dielectric films. Nat. Bur. Stand. (U.S.) Spec. Publ. 435; 1975. 254-271.

[3] Apfel, J. H.; Matteucci, J. S.; Newnam, B. E.; Gill, D. H. The role of electric field strength in laser damage of dielectric multilayers. Nat. Bur. Stand. (U.S.) Spec. Publ. 462, 1976 December. 301-309.

[4] Gill, D. H.; Newnam, B. E; McLeod, J. Use of nonquarter-wave designs to increase the damage resistance of reflectors at 532 and 1064 nanometers. Nat. Bur. Stand. (U.S.) Spec. Publ. 509, 1977 December. 260-270.

[5] Carniglia, C. K.; Apfel, J. H.; Allen, T. H., Tuttle, T. A., Lowdermilk, W. H.; Milam, D.; Rainer, F. Recent damage results on silica/titania reflectors at 1 μm. Nat. Bur. Stand. (U.S.) Spec. Publ. 568; 1979 July. 377-390.

[6] Lowdermilk, W. H.; Milam, D.; Rainer, F. Damage to coatings and surfaces by 1.06 μm pulses. Nat. Bur. Stand. (U.S.) Spec. Publ. 568; 1980 July. 391-403.

[7] Lowdermilk, W. H.; Milam, D. Laser-induced surface and coating damage. IEEE J. Quant. Elect. QE-17 (9) 1888-1903, 1981.

[8] Newnam, B. E.; Gill, D. H. Ultraviolet damage resistance of laser coatings. Nat. Bur. Stand. (U.S.) Spec. Publ. 541; 1978 December. 190-201.

[9] Walker, T. W.; Guenther, A. H.; Fry, C. G., Nielson, P. Pulsed damage thresholds of fluoride and oxide thin films from 0.26 μm to 1.06 μm. Nat. Bur. Stand. (U.S.) Spec. Publ. 568, 1980 July. 405-416.

[10] Apfel, J. H. Optical coating design with reduced electric field intensity. Appl. Opt. 16 (7) 1880-1885; 1977.

[11] Foltyn, S. R., Newnam, B. E. Multiple-shot laser damage thresholds of ultraviolet reflectors at 248 and 308 nanometers. Nat. Bur. Stand. (U.S.) Spec. Publ. 620, 1980 October. 265-276.

[12] Foltyn, S. R.; Newnam, B. E. Ultraviolet damage resistance of dielectric reflectors under multiple-shot irradiation. IEEE J. Quant. Elect. QE-17 (10) 2092-2098; 1981.

[13] Foltyn, S. R; Newnam, B. E.; Jolin, L. J. Laser damage results and analyses for uv reflectors under multiple-shot irradiation. Nat. Bur. Stand. (U.S.) Spec. Publ. (this volume) 1982.

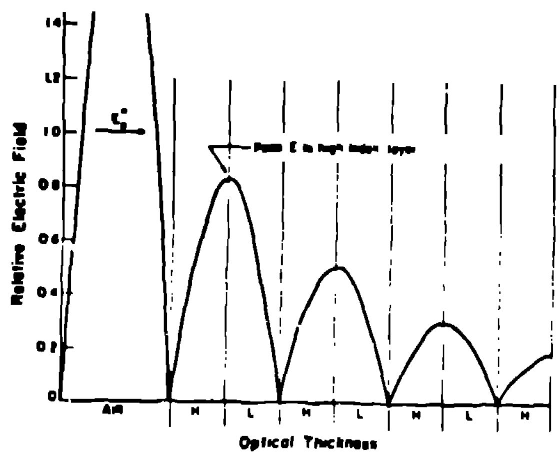

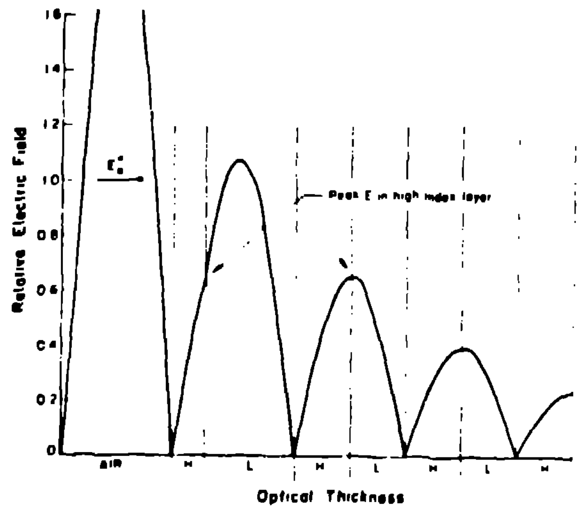

Figure 1. Standing-wave electric-field distribution in two multilayer dielectric reflector designs. E_o^+ is the incident electric field in air. One reflector design (left) uses all QW thicknesses; the other has one pair of non-QW layers optimized for suppression of the peak field in the top H-layer.

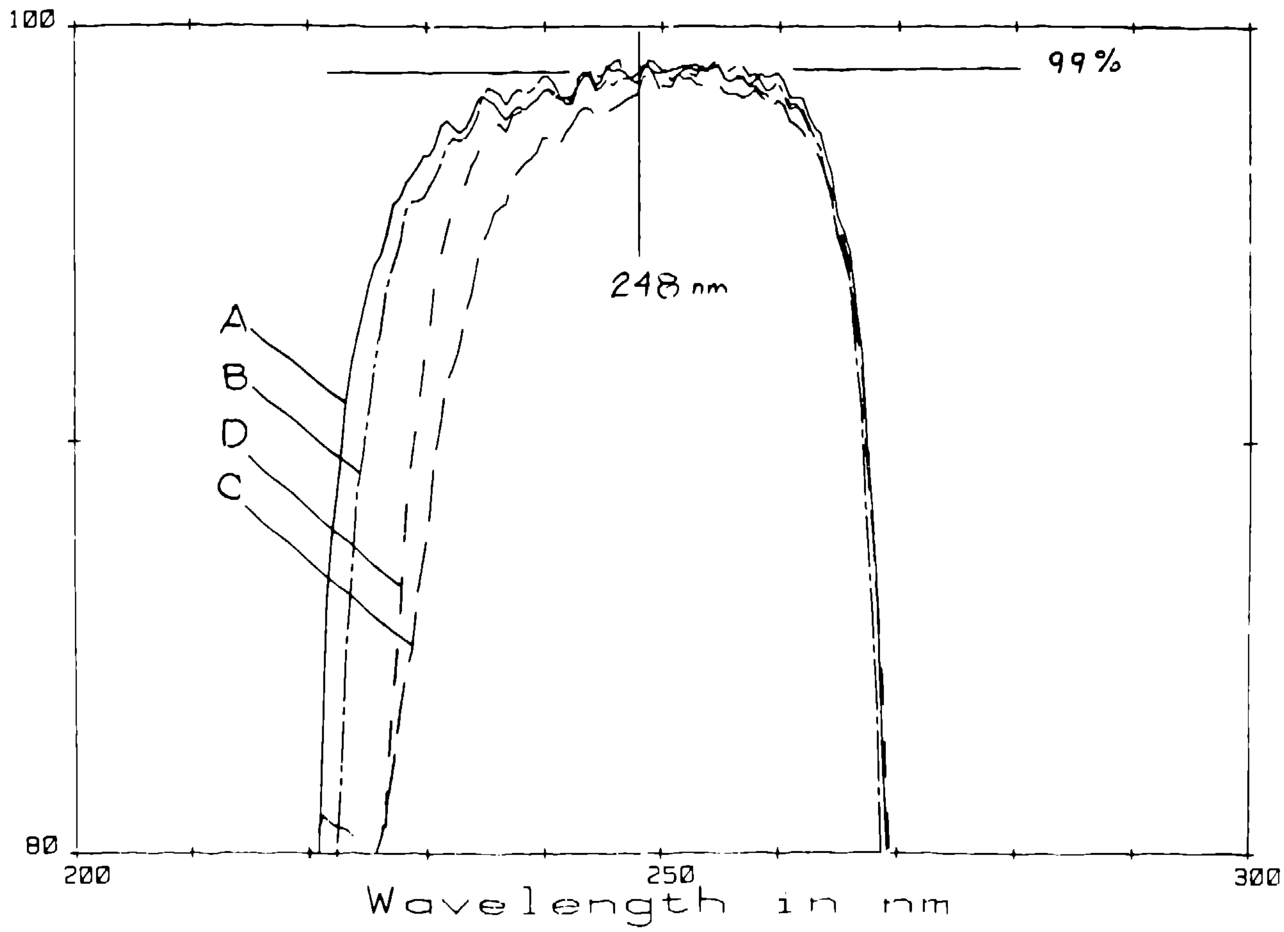

Figure 2. Spectral reflectance (measured) of reflector designs A, B, C, and D.

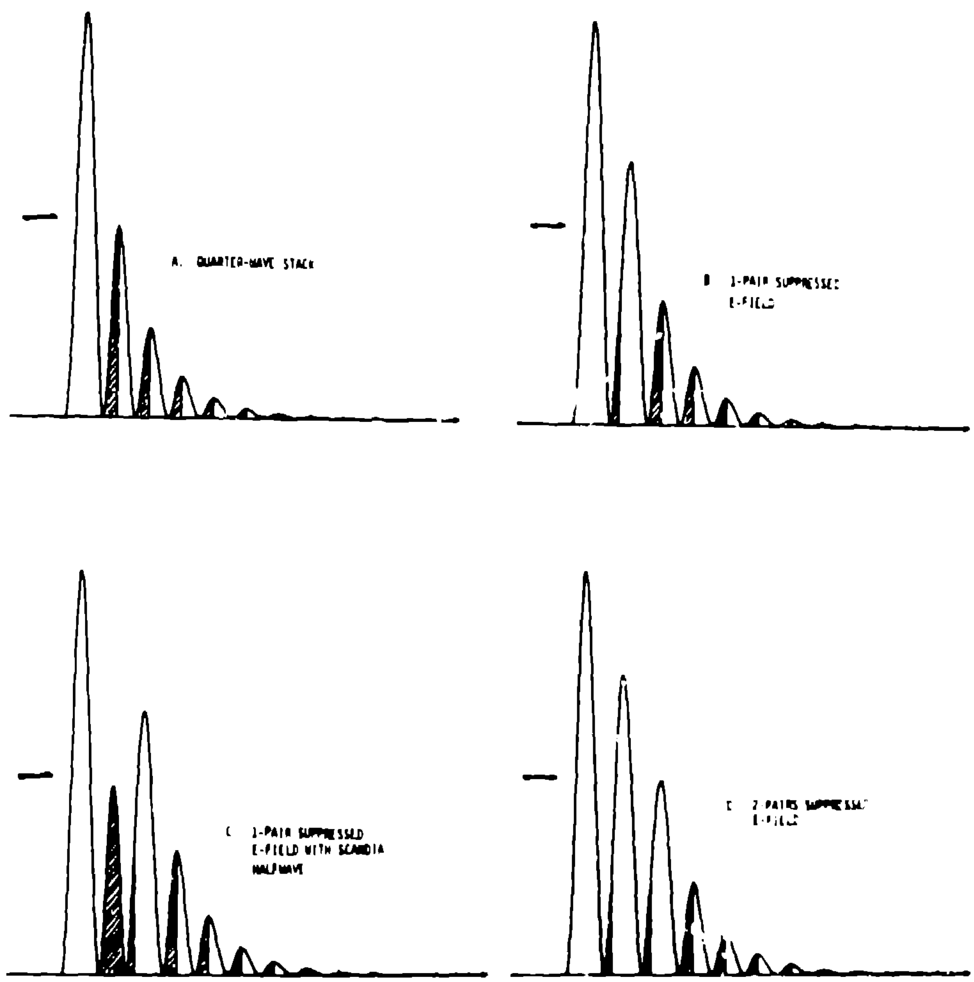

Figure 3. Standing-wave electric field-squared internal to the four reflector designs tested for damage resistance.

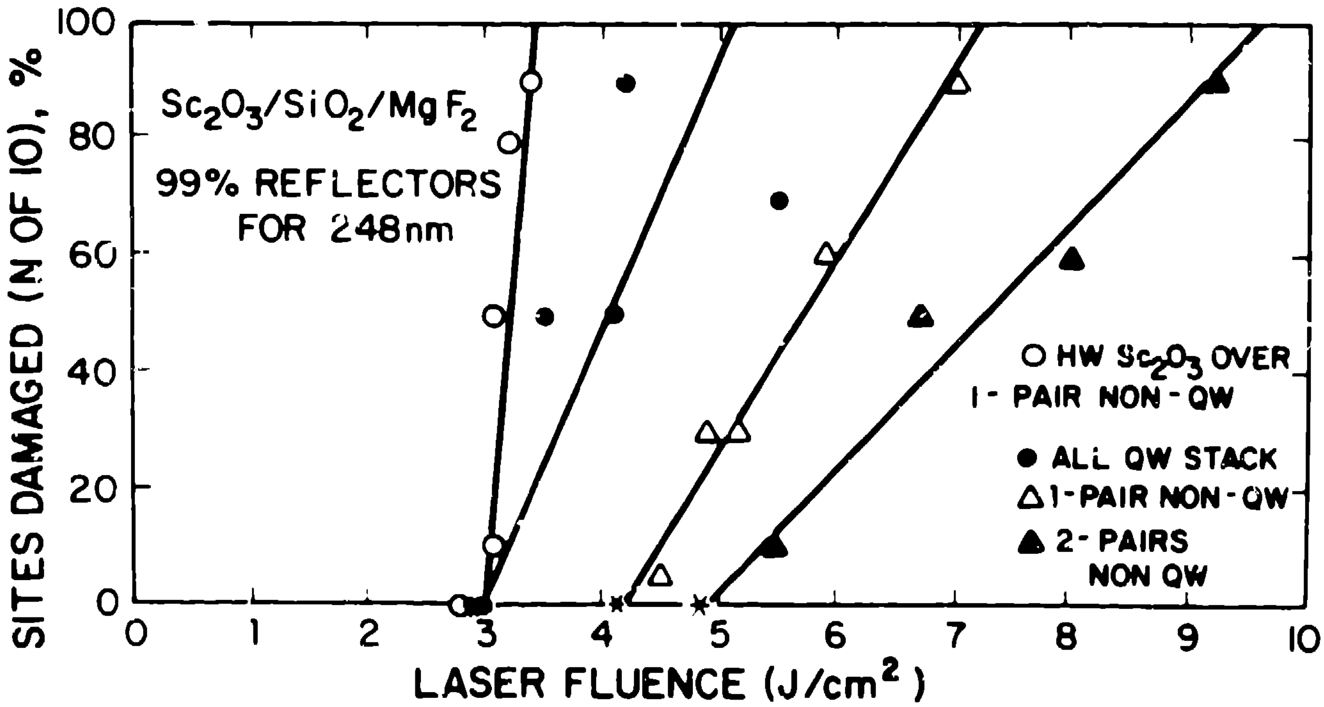

Figure 4 Multiple-shot laser damage test results for one set of reflector designs

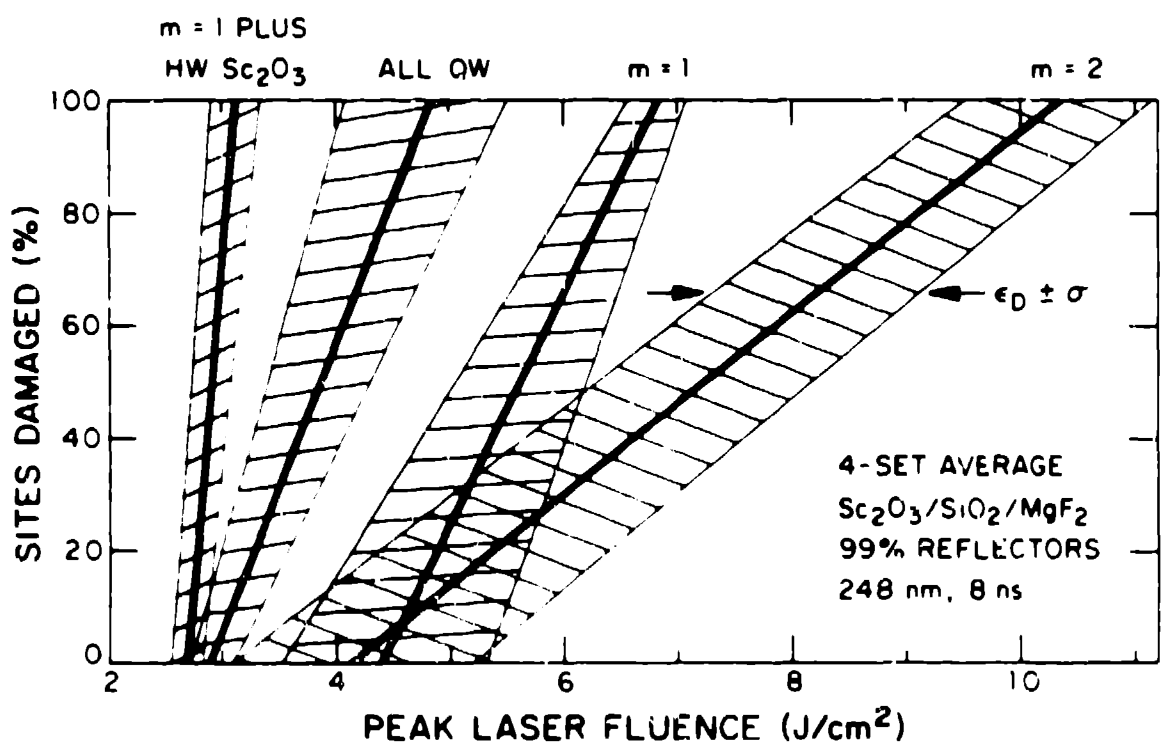

Figure 5. Multiple-shot laser damage test results for four sets of reflector designs. The straight line passes through the mean threshold and saturation fluences, the shaded regions encompass the standard deviations.

ne set of four

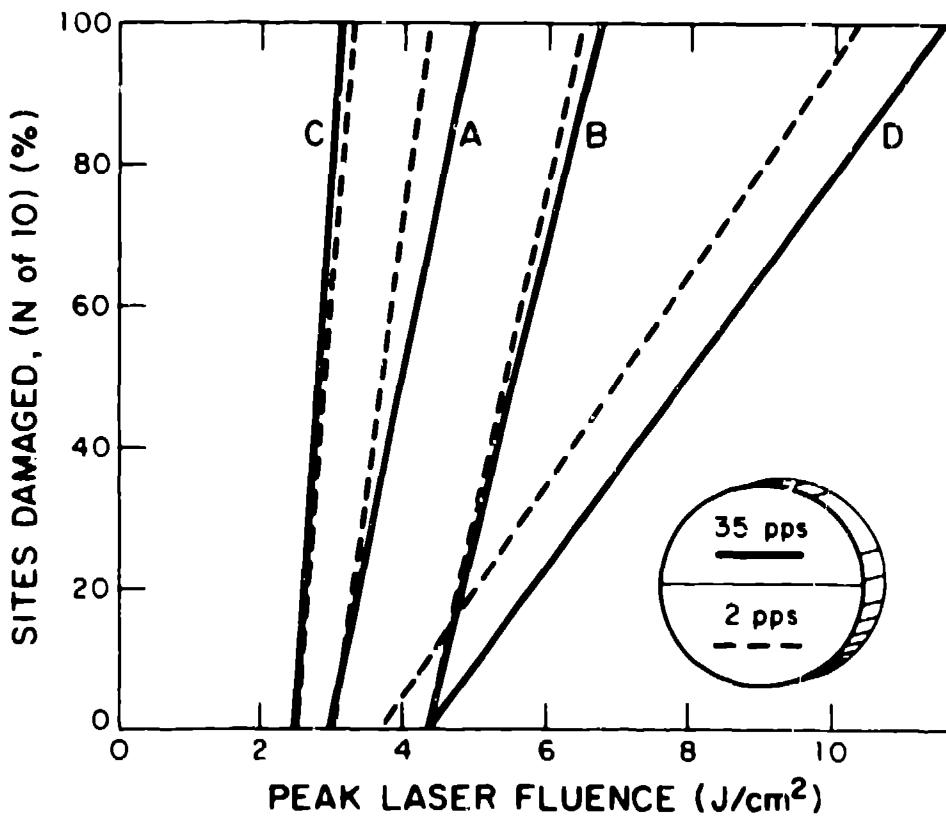

Figure 6 Comparison of multiple shot damage resistance versus repetition rate for o different reflector designs

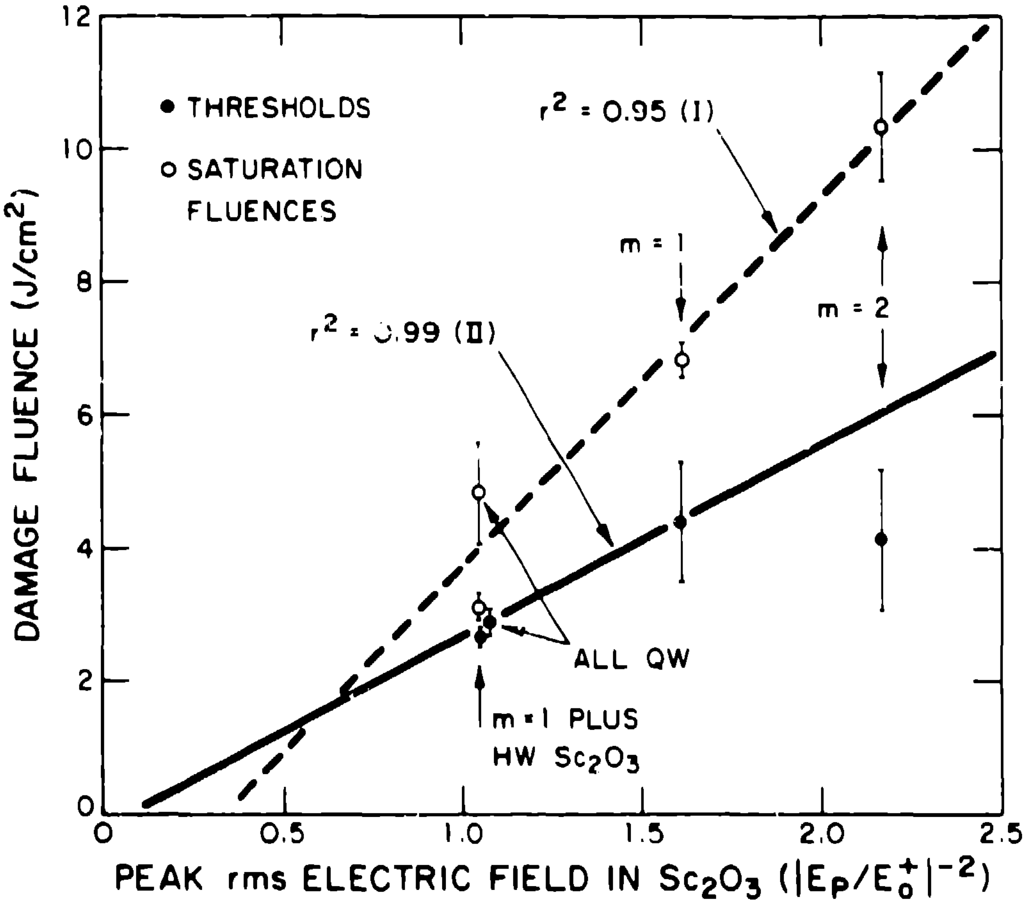

Figure 7. Model 1: Damage fluences versus the inverse of the normalized peak rms electric-field-squared in the scandia layers. Coefficients of determination r^2 indicate the quality of the linear fit to the data according to the hypothesis (I or II) used.

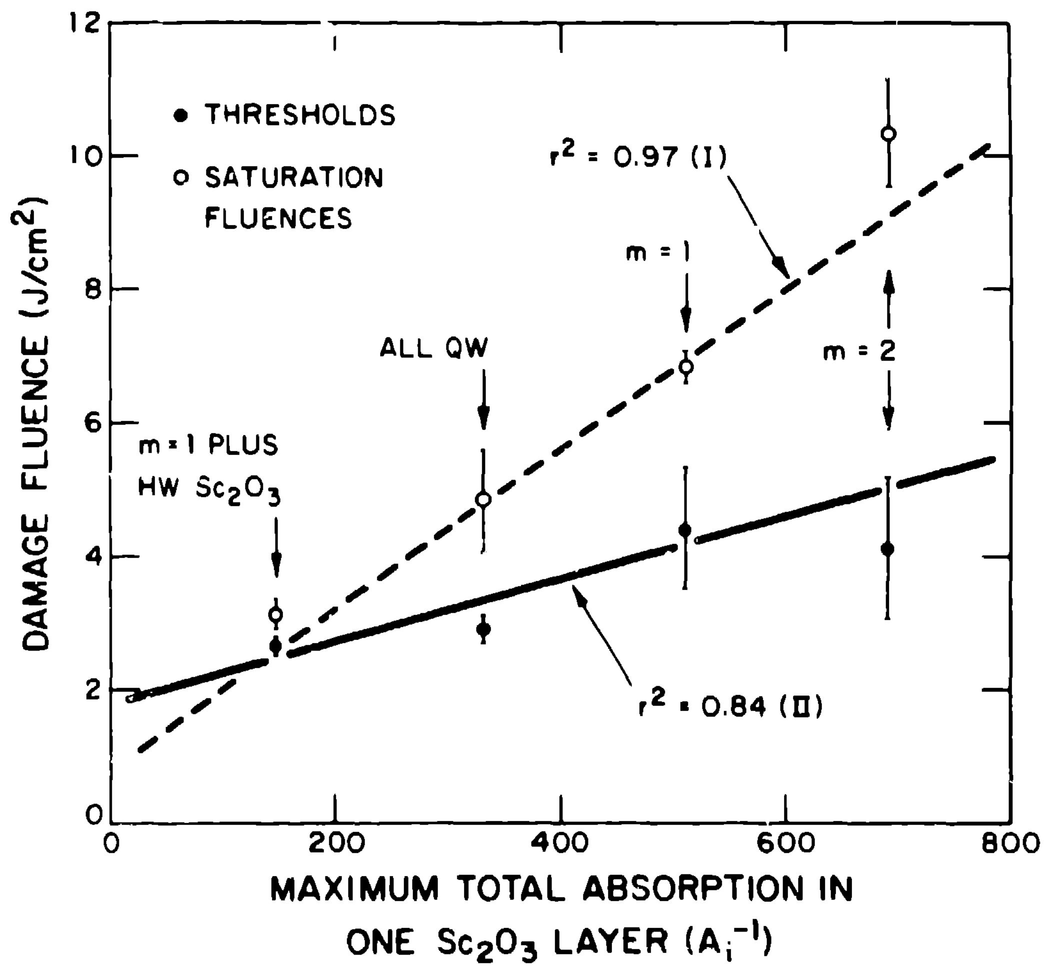

Figure 8. Model 5: Damage fluences versus the inverse of the maximum linear absorption occurring in any single scandia layer.

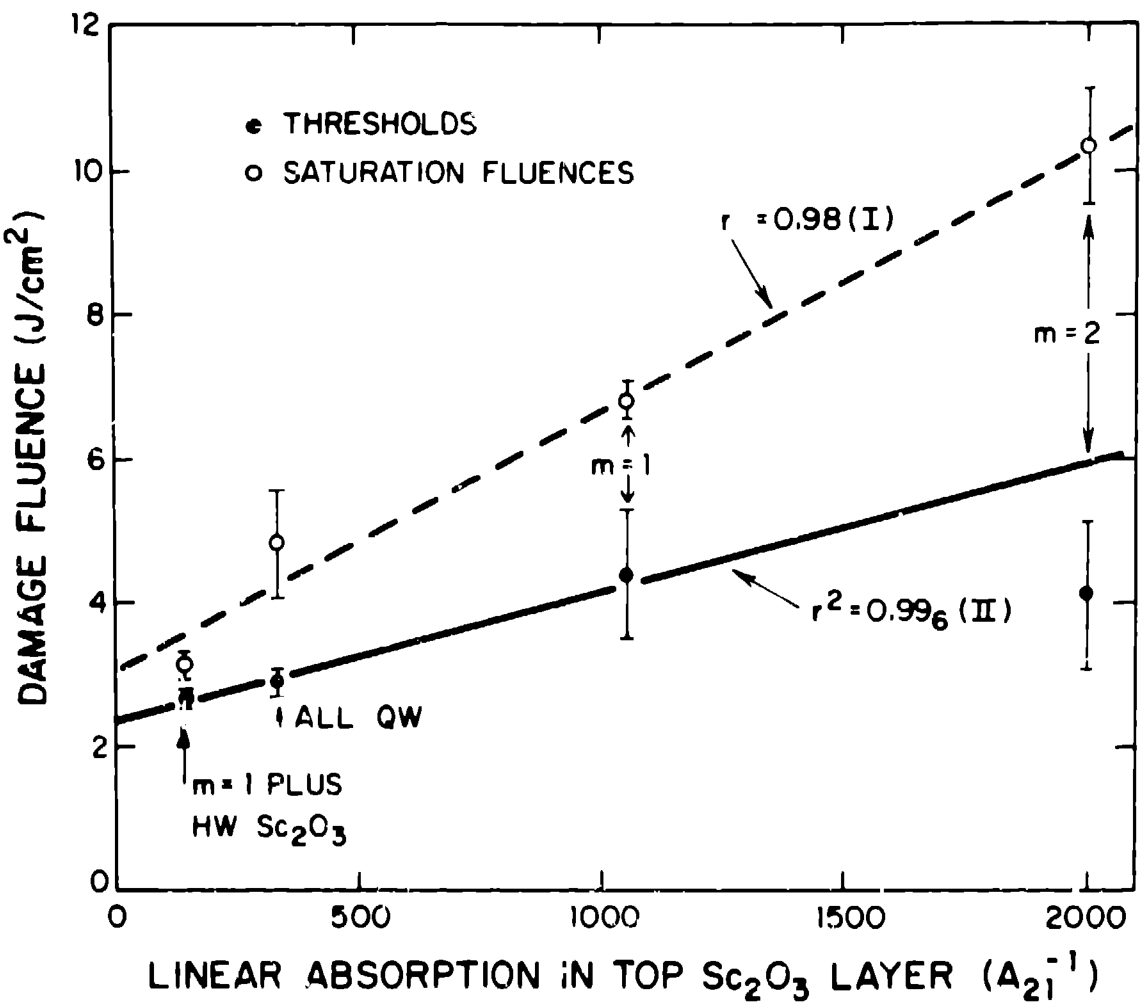

Figure 9. Model 6: Damage fluences versus the inverse of the linear absorption in the top scandia layer

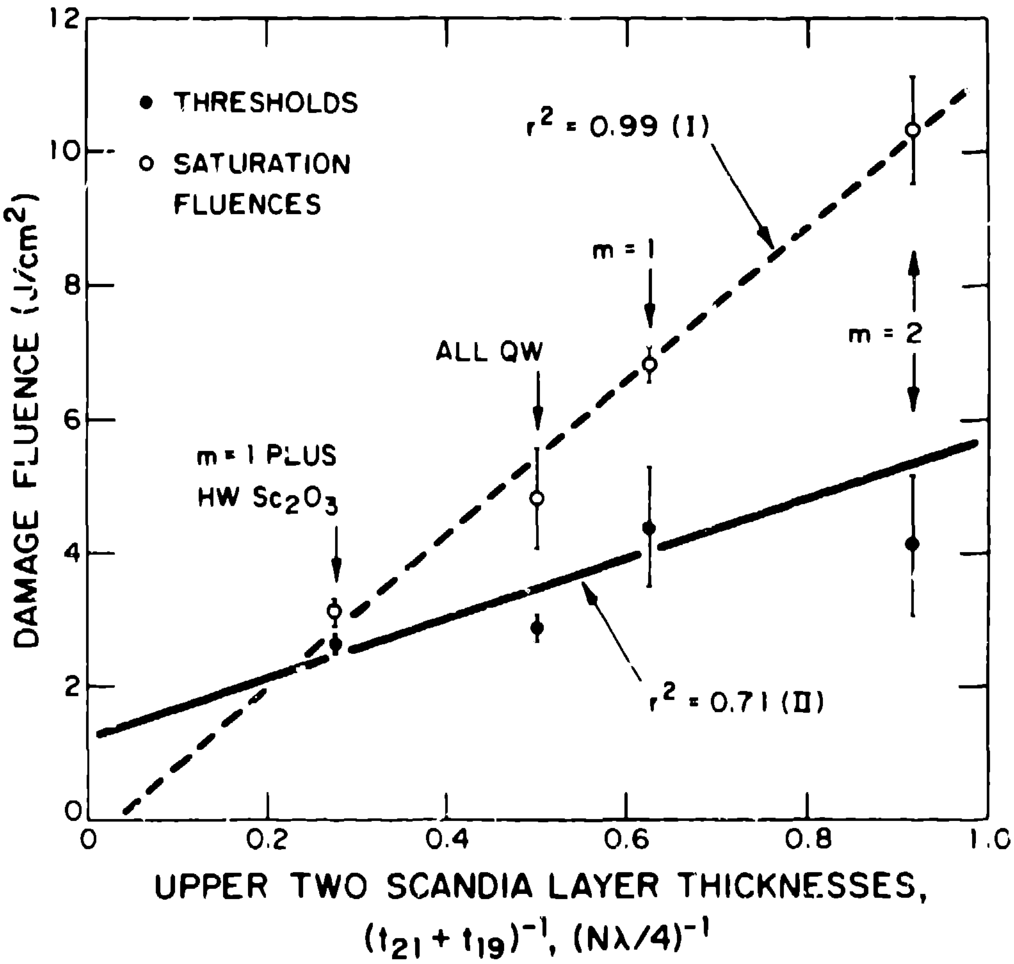

Figure 10. Model 10: Damage fluences versus the inverse of the sum of the thicknesses of the upper two scandia layers.